# A Lentiviral Functional Proteomics Approach Identifies Chromatin Remodeling Complexes Important for the Induction of Pluripotency*[S]

**Anthony B. Mak‡§¶‖, Zuyao Ni‡¶**, Johannes A. Hewel‡¶, Ginny I. Chen§‡‡, Guoqing Zhong‡, Konstantina Karamboulas‡, Kim Blakely‡§, Sandra Smiley‡§, Edyta Marcon‡, Denitza Roudeva‡§, Joyce Li‡, Jonathan B. Olsen‡§, Cuihong Wan‡§, Thanuja Punna‡, Ruth Isserlin‡, Sergei Chetyrkin‡, Anne-Claude Gingras§‡‡, Andrew Emili‡§ §§, Jack Greenblatt‡§¶¶, and Jason Moffat‡§‖‖**

**Protein complexes and protein-protein interactions are essential for almost all cellular processes. Here, we establish a mammalian affinity purification and lentiviral expression (MAPLE) system for characterizing the subunit compositions of protein complexes. The system is flexible (*i.e.* multiple N- and C-terminal tags and multiple promoters), is compatible with Gateway™ cloning, and incorporates a reference peptide. Its major advantage is that it permits efficient and stable delivery of affinity-tagged open reading frames into most mammalian cell types. We benchmarked MAPLE with a number of human protein complexes involved in transcription, including the RNA polymerase II-associated factor, negative elongation factor, positive transcription elongation factor b, SWI/SNF, and mixed lineage leukemia complexes. In addition, MAPLE was used to identify an interaction between the reprogramming factor Klf4 and the Swi/Snf chromatin remodeling complex in mouse embryonic stem cells. We show that the SWI/SNF catalytic subunit *Smarca2*/*Brm* is up-regulated during the process of induced pluripotency and demonstrate a role for the catalytic subunits of the SWI/SNF complex during somatic cell reprogramming. Our data suggest that the transcription factor *Klf4* facilitates chromatin remodeling during reprogramming.** ***Molecular & Cellular Proteomics 9:811–823, 2010.***

The analysis of protein-protein interactions (PPIs)[1] and protein complexes is of central importance to biological research and facilitates our understanding of how molecular events drive phenotypic outcomes. Moreover, large scale protein interaction data can be used to generate protein interaction networks, which can then be used to predict disease genes and model biology in any living organism.

A number of methods (*e.g.* yeast two-hybrid) have been developed to examine binary protein interactions in a systematic format and applied to model systems (1–8). However, affinity purification (AP) coupled with tandem MS has become the method of choice for the identification of protein complexes (9, 10). Large scale PPI studies using a high throughput and systematic AP-MS approach have been performed for *Escherichia coli* (11, 12) and *Saccharomyces cerevisiae* (13–15). In fact, large scale efforts using AP-MS have connected an estimated 60% of the yeast proteome, demonstrating the power of coupling systematic biochemical purifications with mass spectrometry (13–16).

AP-MS has also been used extensively for purification of mammalian protein complexes (17), but this has been mostly restricted to small scale studies and the use of either cell lines that are easy to transfect or highly validated antibodies against specific targets. For example, Glatter *et al.* (18) recently developed an integrated workflow where a high density interactome was developed for the protein phosphatase 2A complex. This workflow relies on "flip-in" technology to introduce transgenes into a common genomic site in HEK293 cells and, similar to work by other groups (19, 20), utilizes an

From the ‡Banting and Best Department of Medical Research, Donnelly Centre, University of Toronto, Toronto M5S3E1, Canada, §Department of Molecular Genetics, Donnelly Centre, University of Toronto, Toronto M5S1A8, Canada, and ‡‡Samuel Lunenfeld Research Institute, Toronto M5T3L9, Canada

Received, January 4, 2010, and in revised form, March 18, 2010

Published, MCP Papers in Press, March 19, 2010, DOI 10.1074/mcp.M000002-MCP201

[1] The abbreviations used are: PPI, protein-protein interaction; MAPLE, mammalian affinity purification and lentiviral expression; AP, affinity purification; IPI, International Protein Index; GFP, green fluorescent protein; eGFP, enhanced green fluorescent protein; VA, versatile affinity; LTQ, linear trap quadrupole; ES, embryonic stem; HEK, human embryonic kidney; MEF, mouse embryonic fibroblast; shRNA, short hairpin RNA; TEV, tobacco etch virus; CMV, cytomegalovirus; hPGK, human phosphoglycerate kinase; mPGK, mouse phosphoglycerate kinase; Ef1$\alpha$, elongation factor 1$\alpha$; Gw, Gateway; qRT-PCR, quantitative RT-PCR; puro, puromycin; hygro, hygromycin; rtTA, reverse tetracycline-controlled transactivator; pLD, plasmid lentiviral destination; pLX, plasmid lentiviral expression; PAF, RNA polymerase II-associated factor; NELF, negative elongation factor; P-TEFb, positive transcription elongation factor b; SWI/SNF, switch/sucrose nonfermentable; MLL, mixed lineage leukemia; VM, V5-Myc; Bis-Tris, 2-[bis(2-hydroxyethyl)amino]-2-(hydroxymethyl)propane-1,3-diol; AQUA, absolute quantification. See supplemental Tables 1–7 for gene names.

inducible promoter to control expression levels of bait proteins (18). Unfortunately, the utility of these approaches is not easily extended to multiple cell types, including primary cells, and a few selected cell types are almost certainly insufficient to recapitulate all biologically relevant protein interactions in mammals. Many protein interactions occur dynamically in distinct cellular contexts and vary with a multitude of factors (*e.g.* embryonic development, tissue type, cell cycle phase, nutrient availability, etc.) that affect epigenetic regulation. Therefore, an efficient strategy for systematic identification of PPI by AP-MS in multiple mammalian cell types (*e.g.* primary diploid and diseased cells) with the potential for integration into a high throughput workflow would be valuable for mapping mammalian protein interaction networks.

Deciphering the chromatin code is arguably the next important milestone in biology. Understanding how all genes are transcribed and regulated in an epigenetic manner will generate cell- and tissue-specific genomic profiles that connect genotype to phenotype. This applies particularly to stem cell biology where somatic cells can be converted to pluripotent cells in a patient-specific manner, providing the raw materials for regenerative medicine. The rapid advances in stem cell research motivated us to develop a system to identify PPI in virtually any mammalian cell type. To this end, we developed an integrated strategy for mammalian functional proteomics with the following features in mind: 1) applicability to most mammalian cell types, 2) compatibility with publicly and commercially available cDNA libraries, and 3) versatility with regard to various affinity purification schemes. To accommodate these features, we combined lentiviral technology (21–23), Gateway™ cloning technology (24), and a unique affinity purification tag including a built-in reference peptide. We then established a functional proteomics workflow for AP-MS. We leveraged this workflow for more than 20 target proteins and multiple cell types, including human cells and primary mouse cells, and benchmarked its utility for identifying PPI and protein complexes related to transcription and chromatin modification.

## EXPERIMENTAL PROCEDURES

### *Cell Culture*

HEK293 and HEK293T cells were cultured in Dulbecco's modified Eagle's medium with 10% fetal bovine serum and antibiotics as described previously (22, 25). Mouse R1 embryonic stem cells were maintained on feeder cells or expanded on gelatin-coated tissue culture plates as described previously (26).

### *Plasmid Construction*

Please refer to supplemental Table 4 for a complete list of plasmids used in this study and supplemental Table 5 for primer sequences used to generate the plasmids in this study.

*Gateway-compatible Entry Clones*—Gateway-compatible entry clones (supplemental Table 4) were obtained by: 1) human ORFeome library (Open Biosystems), 2) UltimateORF collection (Invitrogen), 3) PCR amplification from Mammalian Gene Collection clones to create entry clones into the pDONR223 construct using Gateway BP Clonase enzyme mixture (Invitrogen) according to the manufacturer's protocol, and 4) BP reaction with pMXs (Addgene) expression clones. All entry clones were sequence-verified in full.

*Plasmid Lentiviral Destination (pLD) Vectors*—pLD vectors were all constructed by cloning using T4 DNA ligase (New England Biolabs) according to the manufacturer's protocol. The EF1$\alpha$ promoter was PCR-amplified from pEF_myc_mito (Invitrogen) and cloned into pGateway 5′CMV5′triple FLAG and pGateway 5′CMV3′triple FLAG to generate pGateway 5′EF1$\alpha$5′triple FLAG and pGateway 5′EF1$\alpha$3′triple FLAG. The Ef1$\alpha$ promoter, the Gateway cassette, and either the N- or the C-terminal 3×FLAG tag were PCR-amplified with primers NdeI-EF1a-Gw and EF1a-Ntag-Gw-BstB1_2 or NdeI-EF1a-Gw and EF1a-Gw-Ctag_BstB1_2 from pGateway 5′EF1$\alpha$5′triple FLAG and pGateway 5′EF1$\alpha$3′triple FLAG, respectively, and cloned into the pLKO.1 vector (22) using NdeI/BstBI to generate pLD-puromycin resistance-EF1$\alpha$, N-terminal triple Flag (pLD-puro-EnF) and the corresponding C-terminal triple FLAG construct (pLD-puro-EcF). To efficiently clone in various affinity tags in replacement of the N terminus (5′) 3×FLAG tag flanking NheI/AgeI was introduced by first PCR amplifying the 3×FLAG-$His_6$ (FH) tag[2] with primers PmlI_NheI_FH_F and HindIII_AgeI_FH_R. Then, the PCR-amplified 3×FLAG-$His_6$ tag was digested with PmlI/HindIII and cloned into a pGateway 5′EF1$\alpha$5′triple FLAG first digested by KpnI followed by blunting with DNA polymerase I large (Klenow) fragment (New England Biolabs) according to the manufacture's protocol and then digested with HindIII to generate pLD-puro-EnFH. N- and C-terminal versatile affinity (VA) tags were gene-synthesized (Bio Basic Inc.) with flanking NheI/AgeI and XbaI/BstBI sites, respectively, to allow for subcloning from the pUC57 host vector into pLD-puro-EnFH and pLD-puro-EcF to generate pLD-puro-EnVA and pLD-puro-EcVA, respectively. The CMV promoter from the pLJM1 vector (Addgene) was PCR-amplified using NdeI_hCMV_F and either NheI_hCMV_R or MluI_hCMV_R and cloned into pLD-puro-EnVA and pLD-puro-EcVA using NdeI/NheI or NdeI/MluI to generate pLD-puro-CnVA and pLD-puro-CcVA, respectively. pLD-hygro-EnVM was constructed by subcloning the hygromycin resistance gene from the pLJM6 vector[3] into the pLD-puro-EnFH vector using SpeI/NsiI and subsequently subcloning a gene-synthesized V5-Myc (VM) tag (Bio Basic Inc.) from the pUC57 host vector. The mouse phosphoglycerate kinase (mPGK) promoter was PCR-amplified using primers NdeI-mPGKpr-F and NheI-mPGKpr-R from pMSCV-neo (Clontech) and cloned into pLD-puro-CnVA using NdeI/NheI to generate pLD-puro-PnVA. The tetracycline response element promoter was PCR-amplified from the pLVX-tight-puro (Clontech) using NdeI_Tet_F and either NheI_Tet_R or MluI_Tet_R for N-terminal or C-terminal constructs, respectively, and cloned into pLD-puro-CnVA and pLD-puro-CcVA to generate the intermediary constructs pLD-puro-TnVA and pLD-puro-TcVA, respectively. The rtTA2 was PCR-amplified with primers NheI_rtTA_F and KpnI_rtTA_R and was cloned into pLKO_TRC901 vector (Broad Institute of the Massachusetts Institute of Technology and Harvard University) using NheI/KpnI. PCR-amplified hPGK-pac-2A-rtTA2 was then PCR-amplified using the primers hPGK and NsiI_rtTA and cloned into the pLD-puro-TnVA and pLD-puro-TcVA using SpeI/NsiI to generate pLD-puro-2A-rtTA-TnVa and pLD-puro-2A-rtTA-TcVA, respectively. All DNA fragments cloned into the pLKO.1 backbone vector were sequence-verified in full.

*Plasmid Lentiviral Expression (pLX) Vectors*—pLX vectors were constructed using the Gateway LR Clonase II enzyme mixture (Invitrogen catalog number 11791-020) according to the manufacturer's protocol between Gateway-compatible entry clones and pLD vectors. pLX clones were sequence-verified.

[2] J. Greenblatt, unpublished data.

[3] J. Moffat, unpublished data.

*Stable Cell Lines*

Lentivirus was produced and used to infect either HEK293 or R1 cells at a multiplicity of infection <1 as described previously (22). Transduced cells were selected with puromycin (Sigma) at a concentration of 1 μg/ml for R1 cells and 2 μg/ml for HEK293 for a minimum of 48 h.

*Western Blots and Antibodies*

Cells were subjected to high salt lysis buffer (10 mM Tris-HCl, pH 7.9, 10% glycerol, 420 mM NaCl, 0.1% Nonidet P-40, 2 mM EDTA, 2 mM DTT, 10 mM NaF, 0.25 mM $Na_3VO_4$, and 1× protease inhibitor mixture (Sigma)) by three freeze-thaw cycles as described previously (27) or by radioimmune precipitation assay buffer (50 mM Tris-HCl, pH 7.4, 1% Nonidet P-50 1%, 0.25% sodium deoxycholate, 150 mM NaCl, 1 mM EDTA, 10 mM $Na_3VO_4$, 10 mM sodium pyrophosphate, 25 mM NaF, and 1× protease inhibitor mixture (Sigma)) followed by centrifugation at 14,000 rpm for 1 h at 4 °C to remove insoluble material. 20–100 μg was separated by either a 10% SDS-PAGE gel or a NuPage® Novex® Bis-Tris 4–12% SDS-PAGE gel (Invitrogen) and transferred to nitrocellulose or PVDF membranes. Transferred samples were immunoblotted with primary antibodies (supplemental Table 6), followed by incubation with horseradish peroxidase-conjugated goat anti-mouse or goat anti-rabbit secondary antibodies (Santa Cruz Biotechnology, Inc.). Western blot detection was performed using enhanced chemiluminescence (GE Healthcare). The intensities of protein binds were quantified by Fluor-S™ (Bio-Rad).

*Immunofluorescence*

Cells in 24-well plates were fixed with 4% paraformaldehyde (electron microscopy grade; Electron Microscopy Sciences) followed by permeabilization using 0.2% Triton X-100. Samples were incubated with M2 FLAG antibody at a concentration of 1:1000 (Sigma) at 4 °C overnight. After incubating with goat anti-mouse Alexa Fluor 488- or 647-conjugated secondary antibodies (1:1000; Molecular Probes) and Hoechst 33342 (1:2000; Molecular Probes) for 1 h at room temperature, cells were visualized by microscopy (WaveFX confocal microscope from Quorum Technologies).

*Affinity Purifications*

Lysates for affinity purifications were prepared from 5 × 15-cm plates (HEK293 samples) or 2.5 × 15-cm plates (mouse R1 cells) from stable transgenic cells generated by mammalian affinity purification and lentiviral expression (MAPLE). HEK293 stable transgenic cells were lysed in high salt lysis buffer (described above), and R1 stable transgenic cells were lysed using 50 mM HEPES-KOH, pH 8.0, 10% glycerol, 100 mM KCl, 1% Triton-X, 2 mM EDTA, 2 mM DTT, 10 mM NaF, 0.25 mM $Na_3VO_4$, and 1× protease inhibitor mixture (Sigma) followed by three freeze-thaw cycles. Cells were incubated on ice for a minimum of 30 min and centrifuged at 14,000 rpm at 4 °C for 15 min to 1 h to remove insoluble material. All MAPLE-generated HEK293 samples were purified with FLAG followed by His purifications. MAPLE-generated R1 samples were purified by a sole FLAG purification and by Strep-Tactin followed by FLAG purifications. FLAG purifications were performed as described previously (25). For the FLAG-His purifications, cell lysates were incubated with FLAG M2-agarose beads (Sigma) at 4 °C for 4 h and washed with a low salt lysis buffer followed by tobacco etch virus (TEV) protease cleavage buffer (20 mM Tris-HCl, pH 7.9, 100 mM NaCl, 0.1% Nonidet P-40, and 0.1 mM EDTA) followed by incubation with 0.1 mg/ml TEV protease combined with 2 μg of 3×FLAG peptide (Sigma) at 4 °C overnight. The TEV protease-cleaved products were further incubated with nickel-nitrilotriacetic acid-agarose (Qiagen) at 4 °C for 4 h. After washing with nickel-nitrilotriacetic acid buffer (20 mM Tris-HCl, pH 7.9, 100 mM NaCl, 5 mM imidazole, and 0.1 mM EDTA), proteins were eluted with 500 mM ammonium hydroxide (pH >11). Strep-Tactin-FLAG purifications were performed by incubating cell lysates with Strep-Tactin-Sepharose resin (IBA) at 4 °C for 4 h followed by washes with a low salt wash buffer (10 mM HEPES-KOH, pH 8.0, 100 mM KCl, 0.1% Nonidet P-40, 0.5 mM, and 1 mM DTT). VA-tagged baits were eluted from the Strep-Tactin-Sepharose with 10 mM D-biotin (Sigma) for 30 min and then subjected to the same protocol as FLAG purifications.

*Mass Spectrometry (LC-MS/MS)*

For affinity-purified baits from MAPLE-generated cell lines in HEK293, half of the affinity-purified sample (equivalent to 2.5 × 15-cm plates of HEK293 cells) was precipitated by TCA (final concentration, 20%; Sigma) at 4 °C for overnight followed by cold acetone washing. Samples were then subjected to reduction reaction with 2 mM tris(2-carboxyethyl)phosphine HCl at room temperature for 45 min followed by alkylation reaction with 10 mM iodoacetamide in the dark for 40 min. After the addition of $CaCl_2$ (final concentration, 1 mM), proteins were tryptically digested by using a Sigma Singles kit (T7575) according to the manufacturer's instructions at 37 °C with gentle shaking (1100 rpm) overnight. Digestion was terminated by 1% formic acid (Fluka). 18 μl of 100 μl of digested sample was loaded on a microcolumn using the EASY-nLC system (Proxeon, Odense, Denmark). The microchromatography column was constructed in a 120-mm × 75-μm tip pulled with a column puller (Sutter Instrument, Novato, CA) and packed with 3-μm Luna $C_{18}(2)$ stationary phase (Phenomenex, Torrance, CA). The organic gradient was driven by the EASY-nLC system over 105 min using buffers A and B (98% buffer A (95% water, 5% acetonitrile, and 0.1% formic acid) to 90% buffer B (95% acetonitrile and 0.1% formic acid in water) over 45 min) at a flow rate of 300 nl/min. The gradient was held at 2% B for 1 min followed by a 2-min increase to 6% B, 76-min increase to 26% B, 5-min increase to 90% B, 5-min hold at 90% B, 1-min decrease to 2% B, and 8-min hold at 2% B. Eluted peptides were directly sprayed into an LTQ linear ion trap mass spectrometer (ThermoFisher Scientific, San Jose, CA) using a nanospray ion source (Proxeon). A spray voltage of +2.5 kV was applied. The mass spectrometer was programmed with Xcalibur 2.0 software such that one precursor survey scan was performed for a mass range of *m/z* 400–2000 followed by three data-dependent MS/MS scans selected based on the three most abundant precursor ions and a precursor signal threshold of 500 counts. The exclusion list was enabled to exclude a maximum of 500 ions for 60 s. Overall, there were three biological replicate samples as well as two technical replicate samples to yield six data sets for each bait. Samples were randomized in their analysis so that cross-contamination would be filtered out during data analysis. Moreover, a 30-min wash step was applied between each sample to reduce cross-contamination.

For MS analysis of affinity-purified samples from MAPLE-generated R1 lines, samples were lyophilized in a SpeedVac and trypsin-digested in 50 mM ammonium bicarbonate, pH 8 (0.75 μg for 16 h followed by 0.25 μg for 2 h). The ammonium bicarbonate was removed by SpeedVac, and the samples were resuspended in buffer A (2% acetonitrile and 0.1% formic acid). Then, samples were individually and directly loaded onto capillary columns packed in house with Magic $C_{18}$AQ (5 μm, 100 Å). MS/MS data were acquired from a ThermoFinnigan LTQ equipped with a Proxeon NanoSource and an Agilent 1100 capillary pump via data-dependent mode (over a 2-h 2–40% acetonitrile gradient).

*Analysis of LC-MS/MS Data*

For MAPLE-generated data from HEK293 cells, RAW files were extracted with the extractms program and submitted to database

search using SEQUEST v2.7 and a modified IPI_HUMAN database (version 3.53; 73,748 entries). The modification consisted of adding BSA (Swiss-Prot accession number P02769), GFP (Swiss-Prot accession number P42212), TEV (Swiss-Prot accession number P04517), streptavidin (Swiss-Prot accession number P22629), the beacon peptide (amino acid sequence, ELFNLLGENQPPVVIK), and the reverse sequences of all entries, resulting in a total database size of 147,506 entries. Search parameters were set to allow for one missed cleavage site and one fixed modification of +57 for cysteine using precursor and fragment ion tolerances of 3 and 0 *m/z*, respectively. Protein hits were filtered using the StatQuest program with a confidence level of 99%. Spectral counts were normalized using normalized spectral abundance factors (28) based on protein length and sum of the spectral counts to enable comparison of protein levels across different runs or within a single run. There were 21 independent cell lines (*i.e.* 19 VA-tagged baits and enhanced green fluorescent protein (eGFP) and no tag controls) from which 1916 prey proteins were identified. A two-tailed *t* test was performed on the set of 1916 prey proteins identified by 19 independent baits *versus* the eGFP and no tag controls to filter background contaminants. Significant *p* values ($p < 0.05$) highlighted bait enrichment, and thus these proteins were included in the list. This resulted in a list of 222 confident prey proteins. To add further stringency, preys identified in all three purifications were included in the final analysis set. Lastly, isoforms were removed, and 62 high confidence prey proteins remained. The normalized spectral counts were averaged over the replicate runs to produce an average normalized spectral count for hierarchical clustering. A matrix containing one column for each bait with all its associated preys was produced for all 19 baits. The matrix was clustered using hierarchical clustering with average linkage distance and visualized in Treeview.

For MAPLE-generated data from R1 cells, RAW files were converted into mgf format and were searched using the Mascot search engine (Matrix Sciences) against the Mouse_RefseqV32 database (version 32) in which 35,188 entries were searched. The search parameters included a precursor ion mass tolerance of 3.0 Da and a fragment ion mass tolerance of 0.6 Da. Search parameters were set to allow two missed cleavages and methionine oxidation as a variable modification (fixed modifications were not applicable). Common contaminants associated with FLAG purifications, frequent flyers in mass spectrometry analyses (27), and protein hits found in the VA-tagged GFP samples were removed from the protein hit list. Only protein hits that were detected in all biological replicates, that had a Mascot score greater than 60, and with at least one unique peptide are reported in supplemental Table 3.

### *RNA Interference Experiments*

R1 cells were used to validate lentiviral shRNAs and were infected as described (22). Validation of shRNAs was performed for three biological replicates. The following RNAi Consortium (Sigma-Aldrich) clones were used: shGFP;shGFP-1, shKlf4;shKLF4-1826, shBrg1-1;shBrg1-2260, shBrg1-2;shBrg1-3089, shBrm-1;shBrm-3320, and shBrm-2;shBrm-5135. Knockdowns were allowed to occur for 5 days after the removal of virus. To determine RNA interference knockdown efficiency, cells were processed for both total RNA by TRIzol extraction according to the manufacturer's instructions (Invitrogen catalog number 15596) and total protein determination by radioimmune precipitation assay buffer extraction for qRT-PCR and Western blot analyses, respectively.

### *qRT-PCR*

cDNAs were produced by first strand synthesis from 2 $\mu$g of total RNA according to the manufacturer's instructions (Invitrogen catalog number 11754). Real time PCR using primers for each gene (supplemental Table 7) was performed on a 2-$\mu$l aliquot from a total of 400 $\mu$l of cDNA with the SYBR Green kit (Fermentas catalog number K0221) using the 7300 Real Time OCR System (Applied Biosystems) in a 10-$\mu$l volume in duplicate. PCR consisted of 40 cycles of 95 °C for 15 s and 55 °C for 30 s. A final cycle (95 °C for 15 s and then 60 °C) generated a dissociation curve to confirm a single product. The cycle number required to reach a threshold in the linear range (Qt) was determined and compared with a standard curve for each primer set generated by five 3-fold dilutions of genomic DNA samples of known concentration. Values were normalized to $\beta$-actin. The copy number was determined based on the standard curve generated by running known concentrations of the genomic DNA (1 ng of DNA = 300 copies).

### *Reprogramming Assay*

Secondary mouse embryonic fibroblast (MEF) lines 1B and 6C were maintained and induced to reprogram as described previously (29). Briefly, $2.5 \times 10^4$ MEFs were plated into 12-well plates for the reprogramming assay when overexpressing GFP, Brg1, and Brm by MAPLE. $1.5 \times 10^4$ MEFs were plated into 12-well plates for reprogramming assays after infection with lentiviral shRNAs. We allowed 72 h after lentivirus removal for expression of transgenes or knockdown to occur before the addition of doxycycline. After 7 days, cells were fixed with 4% paraformaldehyde (electron microscopy grade; Electron Microscopy Sciences) and stained with the alkaline phosphatase substrate kit I (Vector Laboratories) according to the manufacturer's protocol. Reprogramming efficiency was scored by counting alkaline phosphatase-positive colonies for three independent assays.

## RESULTS

*MAPLE System*—The MAPLE workflow is outlined in supplemental Fig. 1, and its key features are illustrated in Fig. 1*a*. Briefly, a custom lentiviral plasmid is used to introduce an affinity purification tag onto a given ORF using Gateway recombinant cloning technology (see "Experimental Procedures"). The resulting lentiviral expression constructs are then packaged into lentivirus expression particles, which are used to transduce various types of target cells to create stably expressing cell lines. Protein lysates derived from expanded cell lines are utilized for affinity purifications. Affinity-purified samples are then processed for "gel-free" peptide shotgun sequencing by LC-MS/MS (27). The resulting spectra are used to search sequence databases to identify co-purifying proteins. Because of the broad host range of lentiviruses (22), this procedure can be used to identify PPI and protein complexes in any mammalian cell type that can be amplified to obtain a sufficient amount of cell lysate.

*VA Tag*—Several individual and dual affinity tag combinations incorporating 3×FLAG, $His_6$, Protein G, or Strep III were assessed in a lentiviral context by fusing each tag with the eGFP at either its N or C terminus and determining performance by Western blot analyses, fluorescence microscopy, and binding to appropriate resins (data not shown). Although all the tags that we constructed were functional (as tested by the above mentioned assays), we wanted a flexible solution that could accommodate multiple purification schemes. This motivated us to construct a novel ~12-kDa triple affinity tag,

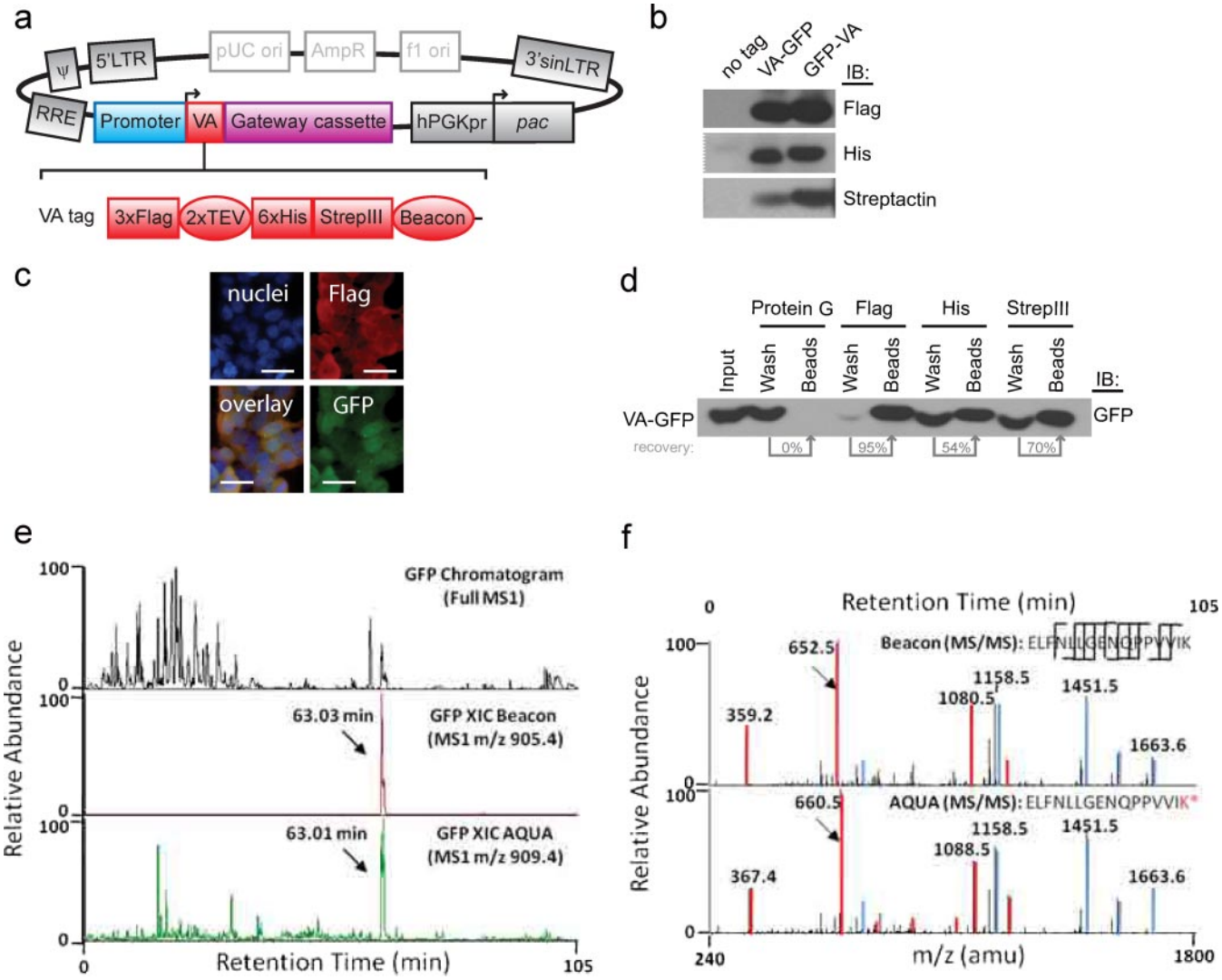


FIG. 1. **MAPLE system.** *a*, schematic representation of the MAPLE lentiviral transfer vector, which includes a mammalian promoter upstream of the VA tag consisting of 3×FLAG separated from $His_6$ and the Strep III tag by dual TEV protease cleavage sites (N-terminal VA tag shown) positioned in-frame with the Gateway cassette. The MAPLE vector also contains the *pac* gene driven by the constitutive human phosphoglycerate kinase (hPGK) promoter. *LTR*, HIV long terminal repeat; *sinLTR*, self-inactivating HIV long terminal repeat; *RRE*, Rev-responsive element; *AmpR*, ampicillin resistance gene. *b*, FLAG, His, and Strep-Tactin epitopes were detected by Western blot analyses of both N- and C-terminally VA-tagged eGFP expressed in HEK293 cells. *c*, the FLAG epitope of the VA tag was used for immunofluorescence of an N-terminally VA-tagged GFP expressed in HEK293 cells. Nuclei were stained with Hoechst. *Bars*, 10 μm. *d*, N-terminally VA-tagged GFP from HEK293 stables is captured by FLAG, nickel, and Strep-Tactin resins but not by Protein G resin. *e*, chromatograms showing the total ion current, extracted ion current (*XIC*) for the beacon (*m/z* 905.4), and extracted ion current for the AQUA-labeled beacon peptide (*m/z* 909.4). *f*, MS/MS spectra of unlabeled beacon at a chromatographic retention time of 63.01 min and AQUA-labeled beacon at a chromatographic retention time of 63.05 min. y-ions are indicated in *red*, and b-ions are shown in *blue*. *IB*, immunoblot.

termed the VA tag, that includes 3×FLAG, $His_6$, and Strep III (30) epitopes for the following reasons. First, 3×FLAG has been widely used, is small in size, and is amenable to immunofluorescence. Second, $His_6$ is widely used and allows for protein purification under denaturing conditions. Third, Strep III is highly selective with little nonspecific binding and efficiently binds to desthiobiotin and biotin for elution (30). The VA tag also contains a dual TEV protease cleavage site (31) and a unique, yeast-derived, high responding proteotypic peptide (ELFNLLGENQPPVVIK) that serves as a molecular "beacon" (32) during mass spectrometry (Fig. 1*a*). Importantly, all three epitopes of the VA tag were easily detected on either the N or C terminus of eGFP by immunoblot (Fig. 1*b*), and VA-GFP localized predominantly to the cytoplasm by GFP fluorescence and anti-FLAG immunofluorescence (Fig. 1*c*). Furthermore, all three epitopes in the VA tag were capable of being captured on appropriate resins with little to no nonspecific adsorption to Protein G beads (Fig. 1*d*).

To confirm bait retrieval, we monitored the abundance of the bait-derived beacon peptide by LC-MS/MS using a heavy

stable isotope-labeled synthetic (*i.e.* AQUA-labeled) reference peptide spiked into the sample digest as an internal standard (supplemental Fig. 2, a and b). As expected, both the unlabeled (*m/z* 905.4) and AQUA-labeled (*m/z* 909.4) beacon peptides co-eluted during liquid chromatography (Fig. 1*e*). The corresponding MS/MS spectra of these precursors revealed a characteristic shift in mass of reporter y-ions (*e.g. m/z* 652.5 → 660.5), demonstrating the potential utility of the AQUA-labeled standard for identifying bait proteins (Fig. 1*f*).

*MAPLE Is an Effective System for Identifying Specific PPIs and Protein Complexes*—To examine an entire complex by reciprocal tagging and validate MAPLE for the characterization of human complexes, we tested the evolutionarily conserved RNA polymerase II-associated factor (PAF) complex as it has been purified previously from human cells and serves as a good control to assess our MAPLE workflow (33, 34). The PAF complex is involved in mediating efficient transcription elongation by RNA polymerase II, mRNA quality control, and chromatin modification that is coupled to transcription elongation (35). The human and yeast PAF complexes contain PAF1, CDC73, CTR9, and LEO1, although the human complex additionally contains SKI8/WDR61 and appears to lack the RTF1 subunit stably associated with the yeast complex at least in some cell types (33, 34, 36). Each of the subunits of the PAF core complex, PAF1, CDC73, CTR9, and LEO1, and RTF1 were VA-tagged and subjected to MAPLE followed by LC-MS/MS to identify a high confidence network of reciprocal protein interactions (18). Importantly, all of these tagged baits were localized to previously reported subcellular compartments, migrated at their predicted molecular weights, and were present at levels comparable with or below the corresponding endogenous proteins (Fig. 2, *a* and *b*). Baits were purified on anti-FLAG and nickel resins and analyzed either by SDS-PAGE followed by silver staining or by trypsin digestion and tandem mass spectrometry to identify potential interacting protein partners. Untagged CDC73 and VA-tagged eGFP were used as negative controls to generate nonspecific background profiles necessary for filtering out common contaminants. Each bait protein was purified from three independent cultures and analyzed twice by data-dependent LC-MS/MS, producing a total of six sample runs per bait.

To score protein-protein interactions, we considered reproducibility and background, and an enrichment score was determined using a combination of protein length-normalized spectral counts and filtering criteria (see below and "Experimental Procedures"). The resulting values were scaled between 0 and 0.01 where 0 represents no preys detected and values over 0.005 were deemed highly significant. The results show that all core members of the human PAF complex consistently co-purified with each of the PAF baits with high enrichment scores (Fig. 2*c*, supplemental Fig. 5, and supplemental Tables 1 and 2). Consistent with the observation by Zhu *et al.* (34), SKI8/WDR61 consistently co-purified with all core members of the PAF complex including PAF1, LEO1, CTR9, and CDC73 and served as a good positive control for our scoring schema and the overall workflow (Fig. 2*c*). Also as expected (34), none of the PAF core components were observed in RTF1 affinity purifications (supplemental Tables 1 and 2) nor were they observed in purifications from cells expressing VA-tagged eGFP or untagged CDC73. However, several preys were weakly captured in common between RTF1 and two PAF-related baits, LEO1 and PAF1, including C17orf79, an uncharacterized human open reading frame, suggesting that there may be some association among these proteins in human cells (supplemental Tables 1 and 2). Overall, the MAPLE workflow permitted the efficient identification of authentic protein complexes in human cells and their rapid validation by reciprocal tagging.

*Systematic Analysis of Protein Complexes Involved in Transcription and Chromatin Modification*—As further validation of the MAPLE workflow, systematic examination of protein complexes involved in various aspects of transcription was performed. The reciprocal tagging strategy used for the PAF complex was again applied to several previously documented multiprotein complexes linked to positive and negative regulation of transcription elongation and chromatin remodeling, including the positive transcription elongation factor b (P-TEFb) (37), negative elongation factor (NELF) (38, 39), mixed lineage leukemia (MLL) (40, 41), and SWI/SNF (42) complexes (Fig. 2*c*, supplemental Fig. 5, and supplemental Tables 1 and 2). A total of 17 proteins representing subunits of the PAF complex and four other complexes as well as PTEN and JUNB were built as baits. Each stably expressing cell line was analyzed by immunoblot and immunofluorescence to confirm that each tagged protein migrated at its predicted molecular weight and localized to the correct subcellular compartment. Each of the baits was purified from HEK293 cells, and its putative interaction partners were identified by LC-MS/MS as described above.

For the NELF complex, all four members of the complex (COBRA1, WHSC2, TH1L, and RDBP) were readily detected as baits and consistently interacted with each other as preys in reciprocal affinity purifications except that TH1L and RDBP did not co-purify when COBRA1 was used as bait (Fig. 2*c*). This suggested that the tag on COBRA1 interfered with its association with TH1L and RDBP and highlighted the value of performing reciprocal experiments with MAPLE to maximize subunit coverage for multiprotein complexes.

The P-TEFb complex, containing the cyclin-dependent kinase CDK9 and its cyclin partner (37), also performed well in reciprocal purifications (Fig. 2*c*). In addition, CDK9 affinity purifications revealed novel potential interactors with obvious functional consequences. One was the CDC37 cochaperone that promotes the association of HSP90 with its protein kinase subset of client proteins to maintain their stability and signaling functions (43). CDC37, HSP90AB1, and HSP90AA2 all co-purified with CDK9 as bait, suggesting that CDK9 could be another client of the CDC37-HSP90 complex.

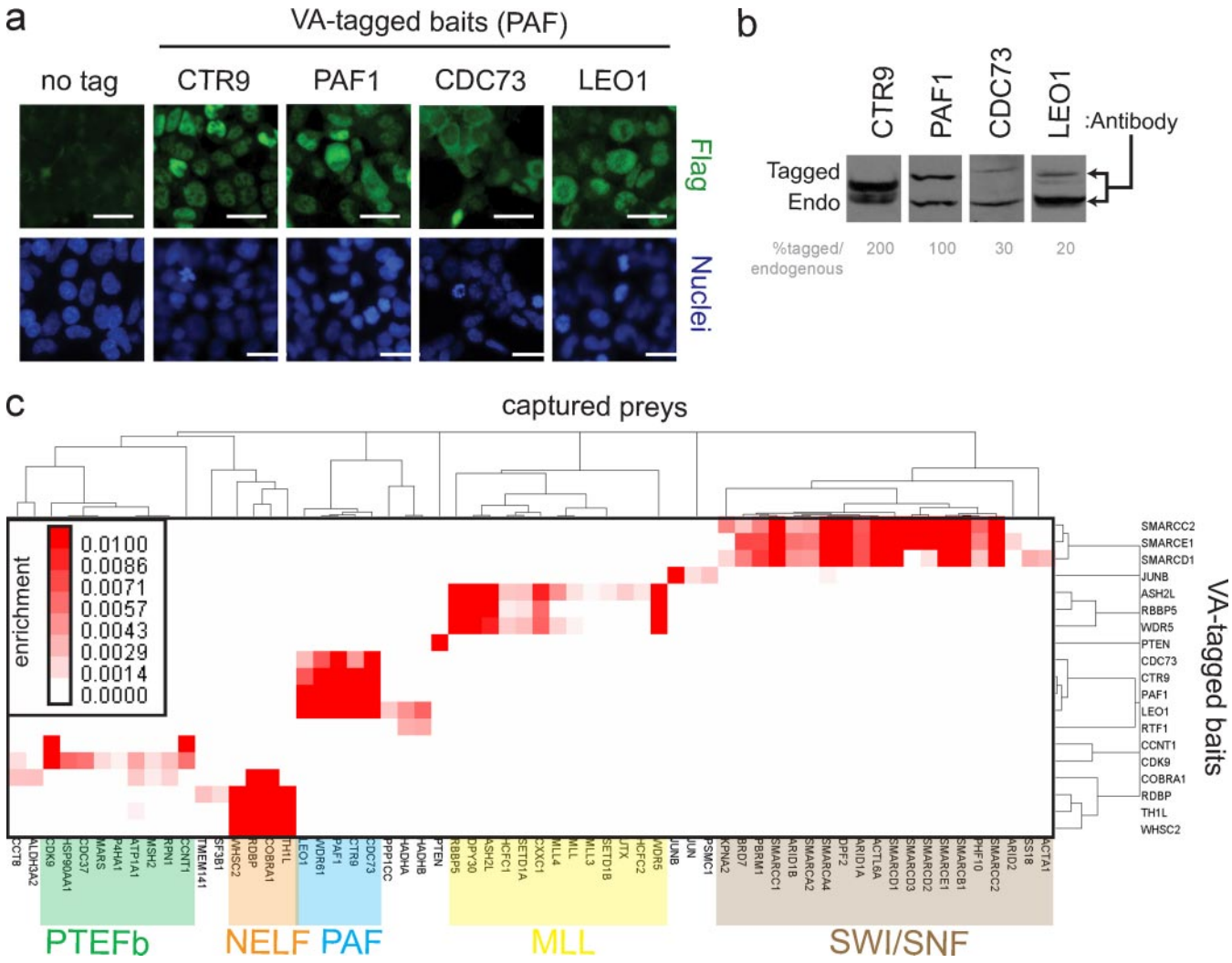


FIG. 2. **MAPLE can reproducibly identify members of known protein complexes.** *a*, subcellular localization by indirect FLAG immunofluorescence of VA-tagged human PAF complex subunits used as baits. Nuclei were stained with Hoechst. *Bars*, 10 $\mu$m. *b*, comparison of expression levels of VA-tagged human PAF complex subunits and their endogenous counterparts by Western blot analyses. *c*, reciprocal MAPLE-LC-MS/MS of members of the human PAF, NELF, P-TEFb, MLL, and SWI/SNF complexes identifies known core complex members as well as potential novel interactions as determined by enrichment scores that indicate significance. Shown is a heat map generated by unsupervised hierarchical clustering of 19 bait proteins spanning five protein complexes that were subjected to MAPLE-LC-MS/MS, including the human PAF, NELF, P-TEFb, MLL, and SWI/SNF complexes.

Likewise, the three members of the MLL histone methyltransferase complex that served as baits (ASH2L, WDR5, and RBBP5) reciprocally co-purified with each other (Fig. 2*c*). The MLL proto-oncogene is a recurrent site of genetic rearrangements in acute leukemias (40). The MLL gene is the founding member of the mammalian SET family of histone-lysine methyltransferases that are responsible for regulating gene expression patterns during development (40). The evolutionarily conserved protein DPY30 also co-purified with each of these baits, consistent with previous evidence that it forms a subcomplex with the ASH2L, RBBP5, and WDR5 proteins that are shared by all human Set1-like histone methyltransferase complexes (44, 45). CXXC1, a protein that recognizes CpG sequences, also co-purified with ASH2L, WDR5, and RBBP5 and is also known to interact with the Set1 histone H3K4-specific methyltransferases in the regulation of MLL target genes (46). Consistent with the notion that ASH2L, WDR5, and RBBP5 form a subcomplex consistently present in MLL complexes, MAPLE purifications revealed interactions with other members of the Set1/COMPASS and MLL complexes, including SETD1A, SETD1B, HCFC1, HCFC2, UTX/KDM6A, MLL, MLL3, and MLL4 (Fig. 2*c*). Further investigation into the nature of these interactions could help refine the composition of these complexes.

The last complex examined by MAPLE in HEK293 cells was the highly conserved SWI/SNF chromatin remodeling complex composed of seven core subunits and one of three different catalytic subunits (BRG1/BAF, BRM/BAF, or PBAF)

(42). Three subunits common to BRG1/BAF, BRM/BAF, and PBAF, namely SMARCC2, SMARCE1, and SMARCD1, were subjected to the MAPLE workflow, and affinity-purified proteins were identified by LC-MS/MS. Affinity capture of all known SWI/SNF subunits was achieved for all three SWI/SNF baits (Fig. 2*c*), and some potential novel interactions were identified as well (Fig. 2*c* and supplemental Tables 1 and 2). For example, DPF2 was identified with all three SWI/SNF baits (Fig. 2*c*). DPF2, also known as REQuiem or UBID4, is a member of the d4 domain family characterized by a zinc finger-like structural motif and may function as a transcription factor important for the apoptotic response (47). This suggests that DPF2 may regulate the role of SWI/SNF during apoptosis.

*MAPLE Synopsis*—In our initial assessment of 19 bait proteins by MAPLE, 1916 prey proteins were identified through LC-MS/MS with one or more spectral counts with a confidence of 99% (corresponding to an false discovery rate of 0.01). Enrichment scores were calculated for each potential prey, yielding a total of 62 high confidence preys representing 148 interactions (see supplemental Fig. 3 for filtering criteria). Unsupervised hierarchical clustering of the baits and high confidence preys indicates that the known subunits of the various complexes share a high measure of similarity and cluster together (Fig. 2*c*). This representation is also a good visualization tool to identify baits that may interact nonspecifically with multiple preys. As described above, our results show good concordance with what has been published in the literature and some overlap with database resources like CORUM, the comprehensive resource of mammalian protein complexes (Ref. 48) and see supplemental Fig. 4). Based on these analyses, we conclude that using MAPLE for reciprocal tagging of known components of large complexes tends to capture the biological diversity of each complex. To examine whether the MAPLE workflow could be applied in a similar fashion to identify protein interactions by AP-MS in a more difficult cell system, we turned to mouse embryonic stem cells.

*Application of MAPLE to Reprogramming Factors*—The OCT4, SOX2, KLF4, and CMYC transcription factors have been shown to cooperatively induce pluripotency in a variety of mouse and human cell types. KLF4, also known as gut-enriched Kruppel-like factor (GKLF), acts as a transcriptional activator or repressor depending on the promoter context and/or cooperation with other transcription factors (49). KLF4 has more recently been shown to cooperate with OCT4, SOX2, and CMYC to induce pluripotency in a variety of mouse and human cell types (50, 51). To examine the utility of MAPLE for investigating protein complexes linked to pluripotency in primary embryonic stem cells, we used the R1 line of mouse ES cells to derive a cell line stably expressing N-terminal VA-tagged KLF4 (Fig. 3*a*). Compared with endogenous protein levels, VA-KLF4 was expressed at levels comparable with its endogenous counterpart (Fig. 3*a*). VA-tagged KLF4 was expressed in the nuclei (Fig. 3*b*), and the VA-KLF4 expressing stable R1 cell line maintained ES cell morphology and ES cell-specific factors (data not shown). Single FLAG purifications and Strep-Tactin-FLAG purifications were performed in parallel followed by LC-MS/MS to identify candidate interacting partners.

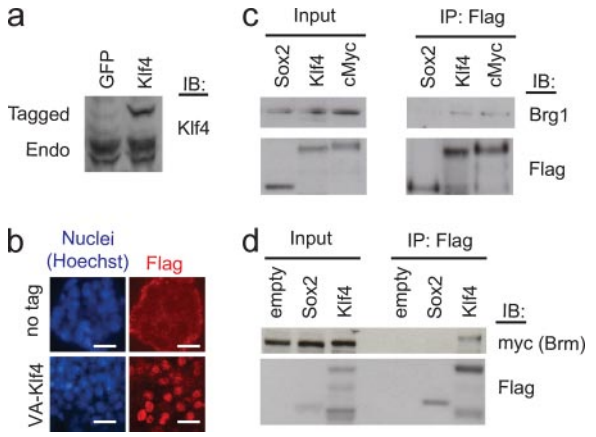


FIG. 3. **KLF4 interacts with SWI/SNF complexes.** *a*, comparison of VA-tagged KLF4 expression level with its endogenous (*Endo*) counterpart in mouse R1 embryonic stem cells as determined by Western blot. *b*, subcellular localization determined by indirect FLAG immunofluorescence of VA-tagged KLF4. Nuclei were detected using Hoechst. *Magnification*, 20×. *Bars*, 5 μm. *c*, VA-SOX2, KLF4, and cMYC from mouse R1 embryonic stem cells were immunoprecipitated using FLAG resin, separated by SDS-PAGE, and transferred to PVDF membranes after which endogenous Brg1 was detected by immunoblotting (*IB*). *d*, HEK293 cells co-transfected with vectors encoding VA-SOX2 or KLF4 as well as VM-SMARCA2/BRM were analyzed by immunoprecipitation (*IP*)/Western blot as in *c*.

Several novel KLF4 protein interactors were identified, including the catalytic subunits SMARCA4/BRG1 and SMARCA2/BRM of the SWI/SNF chromatin remodeling complex (supplemental Table 3 and supplemental Fig. 6). Using a co-immunoprecipitation assay, the interaction between the KLF4 bait and endogenous SMARCA4/BRG1 was validated in mouse embryonic stem cells (Fig. 3*c*).The interaction between KLF4 and SMARCA2/BRM was validated by co-immunoprecipitation in HEK293 cells (Fig. 3*d*). In addition, the c-Myc bait was able to co-immunoprecipitate endogenous SMARCA4/BRG1 in mouse ES cells (Fig. 3*c*), validating a KLF4-SMARCA4/BRG1 interaction previously reported in a high throughput AP-MS study in human cancer cells (17). Taken together, these data indicate that KLF4 interacts, directly or indirectly, with the catalytic subunits SMARCA4/BRG1 and SMARCA2/BRM of the SWI/SNF chromatin remodeling complex in pluripotent stem cells.

*Requirement for SWI/SNF during Induction of Pluripotency*—A direct link between the SWI/SNF chromatin remodeling complex and somatic cell reprogramming has not been clearly established. Because *Klf4* is important for induced pluripotency (50, 51) and we observed an association between KLF4 and the SWI/SNF complex in mouse ES cells, the

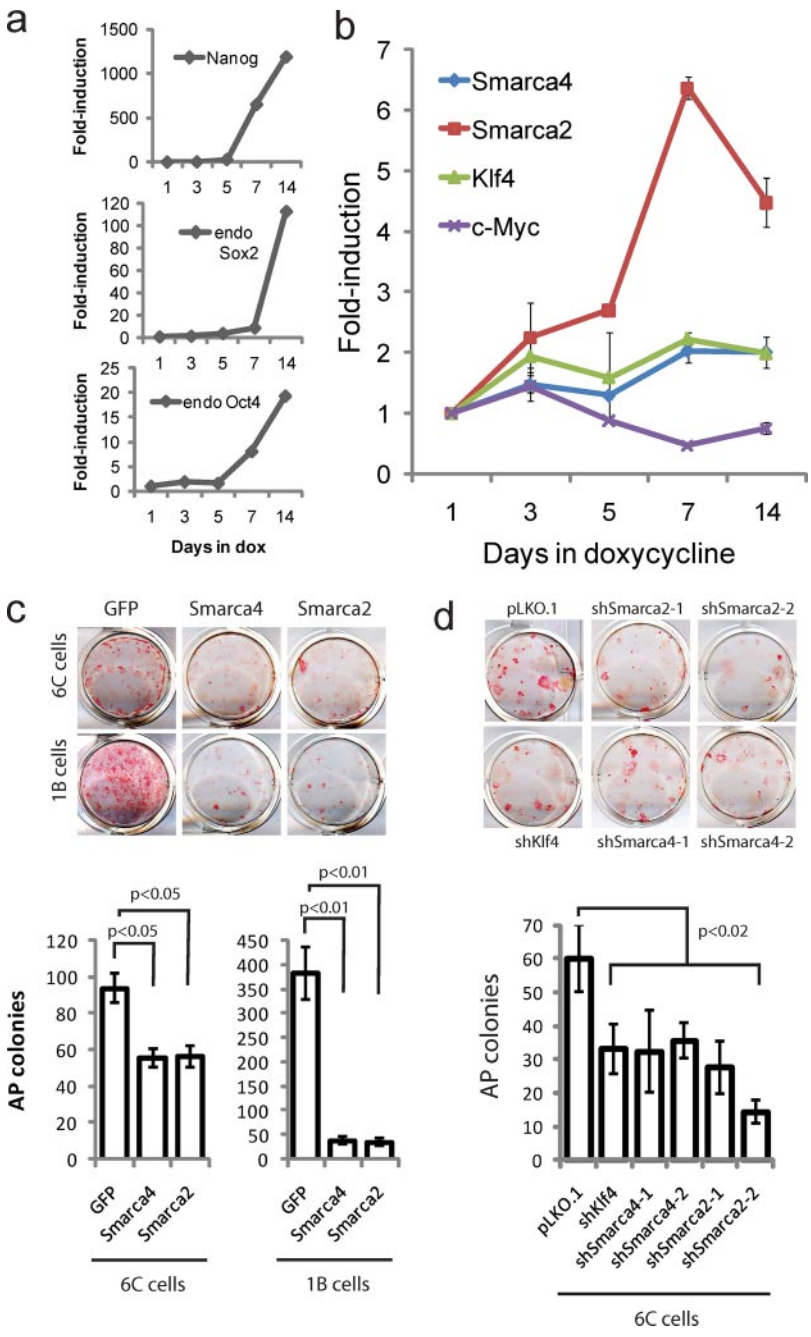


FIG. 4. **SWI/SNF requirement during induction of pluripotency.** *a*, endogenous (*endo*) *Oct4*, *Sox2*, and *Nanog* RNA levels were monitored by qRT-PCR at days 1, 3, 5, 7, and 14 after the addition of doxycycline to 6C secondary MEF cells. *b*, *Klf4*, *Brg1*, and *Brm* RNA levels were monitored in the same manner as in *a*. *c*, alkaline phosphatase (*AP*)-stained colonies in doxycycline-induced 1B or 6C secondary MEFs after 7 days following expression of BRG1 or BRM using MAPLE. *Error bars* represent standard error ($n = 3$). *d*, results of knocking down KLF4, BRG1, or BRM using lentiviral shRNAs in secondary 6C MEF cells following forced expression of *Oct4*, *Sox2*, *Klf4*, and c-*Myc* by addition of doxycycline ($n = 3$). The number of alkaline phosphatase-positive colonies was manually counted by three independent observers, and results were averaged. *Error bars* represent standard error ($n = 3$).

question is raised whether the SWI/SNF-mediated chromatin remodeling contributes to the process of induced pluripotency. To test this idea, we used an established reprogramming assay comprising secondary MEFs that can be converted into induced pluripotent stem cells by addition of doxycycline (29). To examine the efficiency and kinetics of reprogramming in the secondary MEF lines 1B and 6C after doxycycline was added to induce reprogramming, samples were taken to examine expression of pluripotency markers. In parallel, high resolution video microscopy was performed on 6C cells to observe induced pluripotent stem colony formation (supplemental Fig. 7). The expression of the pluripotency markers *Oct4*, *Nanog*, *Eras*, *Zfp42*, *Nrob1*, and *Fbx15* was evident 7 days following addition of doxycycline, whereas the expression of *Sox2* and *Foxd3* was delayed but established by day 15 (Fig. 4*a* and data not shown). The expression of *Smarca4*/*Brg1* increased ~2-fold over the course of the reprogramming assay, whereas surprisingly *Smarca2*/*Brm* expression increased up to ~7-fold (Fig. 4*b*). These observations suggest that *Smarca2*/*Brm*, along with *Smarca4*/*Brg1*, may have an important role in reprogramming/dedifferentiation and possibly establishment of pluripotency.

To assess the requirement of *Smarca4/Brg1* and *Smarca2/Brm* during reprogramming, we perturbed their expression levels in either 6C or 1B cells by using lentiviral cDNAs (overexpression) or short hairpin RNAs (knockdown) (supplemental Fig. 8). Cells were induced to reprogram, and the efficiency was scored based on the number of alkaline phosphatase-positive colonies after 7 days. Lentivirus-mediated expression of GFP or the pLKO.1 vector did not significantly alter the number of alkaline phosphatase-positive colonies compared with the untransduced control (data not shown). In contrast, overexpression of *Smarca4/Brg1* or *Smarca2/Brm* reduced the number of alkaline phosphatase-positive colonies formed from 6C cells by ~2-fold ($p < 0.05$) and the number of alkaline phosphatase-positive colonies formed from 1B cells by ~7-fold ($p < 0.01$) (Fig. 4*c*). Furthermore, knockdown of *Smarca4/Brg1* or *Smarca2/Brm* with either of two independent shRNAs reduced the number of alkaline phosphatase-positive colonies formed from 6C cells by ~2-fold ($p < 0.02$) (Fig. 4*d*). Taken together, these results indicate that the catalytic subunits of the SWI/SNF chromatin remodeling complex, likely in association with KLF4, are important for somatic cell reprogramming.

## DISCUSSION

The goal of this study was to design a system to facilitate identification of protein complexes in a wide variety of mammalian cell types. To this end, we developed MAPLE and coupled it to tandem mass spectrometry to identify protein complexes. MAPLE works efficiently with most cell types, thereby granting access to cell types that may better recapitulate the natural environment of a protein complex. This could be particularly important in cells and tissues that undergo substantive epigenetic regulation such as stem cells. MAPLE is based on a custom-built lentiviral plasmid that is Gateway-compatible and relies on commercially available cDNA libraries. A unique and versatile affinity tag (*i.e.* VA) was created to accommodate different purification schemes and to contain a novel yeast proteotypic peptide (*i.e.* beacon) that acts as a reference for the bait during affinity purifications. As such, the beacon serves as a "digital Western."

A major disadvantage of mammalian AP-MS approaches is the amount of starting material (*i.e.* cells) required to achieve high protein purification yields. Although the original tandem affinity purification tag (52) is still routinely in use in mammalian cells for protein complex characterization, other affinity tags like the GS tag have helped reduce the amount of starting material required by 10–100-fold (53). With the MAPLE system, we typically used ~5*e*7 cells for starting material, similar to Bürckstümmer *et al.* (53). The VA tag is compatible with single, dual, or even triple affinity purification schemes so the choice of method will impact how much starting material is required. That is, more purification steps require more starting material. The downfall of tandem purification methods is that transient or weak interactions are generally lost.

Furthermore, we introduced a constitutive promoter in our MAPLE system and demonstrated that the CMV and PGK promoters driving cDNAs in HEK293 and R1 cells, respectively, resulted in bait expression levels comparable with endogenous. However, some genes or cells may be sensitive to bait overexpression, resulting in false outcomes. Similar to other studies, we demonstrate that MAPLE can be adapted to be tetracycline-regulatable and -inducible (supplemental Fig. 9). Although determining an optimal level of bait expression would be ideal, it is not practical for a systematic and high throughput approach.

To benchmark the MAPLE workflow in cells that are easy to manipulate, we examined 19 bait proteins involved in different aspects of chromatin biology or disease in HEK293 cells. Except for the PTEN phosphatase and the JUNB proto-oncogene, each of the baits was part of an evolutionarily conserved multiprotein complex. PAF1, CDC73, CTR9, and LEO1 represent evolutionarily conserved core components of the human PAF complex involved in transcription elongation. CDK9 and CCNT1 constitute the P-TEFb complex. COBRA1, WHSC2, TH1L, and RDBP represent the core components of the NELF complex. WDR5, RBBP5, and ASH2L make up a key subcomplex that likely regulates all the SET-like histone methyltransferase complexes, including SET1 and all MLL proteins. Lastly, SMARCD1, SMARCC2, and SMARCE1 are common components of all three characterized SWI/SNF chromatin remodeling complexes, including BRG/BAF, BRM/BAF, and PBAF. Importantly, reciprocal tagging validated all the known protein complexes in our benchmarking study, and thus it represents a good strategy to capture new complex members. The application of MAPLE and LC-MS/MS across a broad range of baits in an unbiased manner will yield a high density protein interaction data set with a wealth of new biological information.

A key feature of the MAPLE system is that lentiviruses are efficient at stably transducing most cell types. By transducing cells at a low multiplicity of infection, one can limit the number of integrants per cell and keep cell-to-cell expression levels more constant. The fact that the resulting populations of cells are heterogeneous because of variability in integration is advantageous as this mitigates the possibility of bias due to clonal expansion. To put this to the test, we generated stable mouse R1 ES cells expressing VA-tagged KLF4, one of the classical reprogramming factors that convert somatic cells into induced pluripotent stem cells (51) and performed AP-MS using lysates from this stable cell line to identify protein interactions. We were able to show that KLF4 interacts with the SWI/SNF chromatin remodeling complexes containing SMARCA4/BRG1 and SMARCA2/BRM.

Consistent with this, recent studies have found that ES cells contain a functionally and structurally specialized chromatin remodeling complex, esBAF, that is critical for the self-renewal of ES cells and maintenance of the stem cell fate (54–57). In fact, Crabtree and co-workers (56) proposed that

the surface of esBAF complexes is tailored for interactions with factors found specifically in ES cells and that through these functional interactions esBAF maintains the pluripotent chromatin landscape. Using chromatin immunoprecipitation coupled with high throughput sequencing technology, Ho *et al.* (55) were able to demonstrate that esBAF is enriched at transcription start sites, occupies genes of the core pluripotency network (*i.e. Oct4*, *Sox2*, and *Nanog*), represses developmental genes, and opposes Polycomb complexes by direct repression of subunits of the PRC1 complex. Nevertheless, a direct role for esBAF or any of the SWI/SNF complexes in reprogramming or dedifferentiation had not been shown.

Because KLF4 has an important role during somatic cell reprogramming to induced pluripotent stem cells and our data uncovered an interaction between KLF4 and the catalytic subunits of the SWI/SNF chromatin remodeling complexes, an important remaining question was to examine the requirement of SWI/SNF chromatin remodeling complexes during somatic cell reprogramming. Thus, we turned to a model where secondary MEFs can be induced to pluripotency by the addition of doxycycline (29). The first clue that somatic cell reprogramming may have a slightly different SWI/SNF requirement than maintenance of the pluripotent state (55, 56) came from the observation that SMARCA2/BRM expression is induced during reprogramming/dedifferentiation (Fig. 4*b*). This observation may have important consequences for how SWI/SNF subunits are distributed during reprogramming *versus* maintenance of pluripotency or self-renewal. To further investigate this, the onset of the expression of pluripotency markers was examined in two independent clones (1B and 6C) that were induced into pluripotency following knockdown or overexpression of SWI/SNF catalytic subunits (*i.e.* SMARCA4/BRG1 or SMARCA2/BRM). These results indicate that slight changes in the concentrations of the catalytic subunits of the esBAF (or any SWI/SNF complex involved in reprogramming) complex have drastic consequences for reprogramming to the pluripotent state. The interaction between KLF4 and SWI/SNF complexes may help to establish the pluripotent transcriptional circuitry.

*Acknowledgments*—We thank Dr. Andras Nagy for kindly providing the R1 mouse ES cell line, the 1B and 6C secondary MEFs, and the pDONR221-Klf4 construct and Dr. Tony Pawson for the pGateway vectors. We thank Drs. Anthony Gramolini, Stephane Angers, Janet Rossant, and Brian Cox for helpful discussions.

* This work was supported in part by grants from the Canadian Institutes of Health Research (to J. M. (Grant 178975), J. G., and A. E.) and in part by a Network Centers of Excellence Stem Cell Network grant (to J. M.).

S This article contains supplemental Figs. 1–9 and Tables 1–7.

¶ These authors contributed equally to this work.

‖ Supported by a Natural Sciences and Engineering Research Council Canada graduate scholarship.

** Supported by a Canadian Institutes of Health Research postdoctoral fellowship.

§§ To whom correspondence may be addressed. Tel.: 416-978-0336; Fax: 416-978-8287; E-mail: andrew.emili@utoronto.ca.

¶¶ To whom correspondence may be addressed. Tel.: 416-978-0336; Fax: 416-978-8287; E-mail: jack.greenblatt@utoronto.ca.

‖‖ To whom correspondence may be addressed. Tel.: 416-978-0336; Fax: 416-978-8287; E-mail: j.moffat@utoronto.ca.

REFERENCES

1. Braun, P., Tasan, M., Dreze, M., Barrios-Rodiles, M., Lemmens, I., Yu, H., Sahalie, J. M., Murray, R. R., Roncari, L., de Smet, A. S., Venkatesan, K., Rual, J. F., Vandenhaute, J., Cusick, M. E., Pawson, T., Hill, D. E., Tavernier, J., Wrana, J. L., Roth, F. P., and Vidal, M. (2009) An experimentally derived confidence score for binary protein-protein interactions. *Nat. Methods* **6,** 91–97
2. Giot, L., Bader, J. S., Brouwer, C., Chaudhuri, A., Kuang, B., Li, Y., Hao, Y. L., Ooi, C. E., Godwin, B., Vitols, E., Vijayadamodar, G., Pochart, P., Machineni, H., Welsh, M., Kong, Y., Zerhusen, B., Malcolm, R., Varrone, Z., Collis, A., Minto, M., Burgess, S., McDaniel, L., Stimpson, E., Spriggs, F., Williams, J., Neurath, K., Ioime, N., Agee, M., Voss, E., Furtak, K., Renzulli, R., Aanensen, N., Carrolla, S., Bickelhaupt, E., Lazovatsky, Y., DaSilva, A., Zhong, J., Stanyon, C. A., Finley, R. L., Jr., White, K. P., Braverman, M., Jarvie, T., Gold, S., Leach, M., Knight, J., Shimkets, R. A., McKenna, M. P., Chant, J., and Rothberg, J. M. (2003) A protein interaction map of Drosophila melanogaster. *Science* **302,** 1727–1736
3. Ito, T., Tashiro, K., Muta, S., Ozawa, R., Chiba, T., Nishizawa, M., Yamamoto, K., Kuhara, S., and Sakaki, Y. (2000) Toward a protein-protein interaction map of the budding yeast: A comprehensive system to examine two-hybrid interactions in all possible combinations between the yeast proteins. *Proc. Natl. Acad. Sci. U.S.A.* **97,** 1143–1147
4. Li, S., Armstrong, C. M., Bertin, N., Ge, H., Milstein, S., Boxem, M., Vidalain, P. O., Han, J. D., Chesneau, A., Hao, T., Goldberg, D. S., Li, N., Martinez, M., Rual, J. F., Lamesch, P., Xu, L., Tewari, M., Wong, S. L., Zhang, L. V., Berriz, G. F., Jacotot, L., Vaglio, P., Reboul, J., Hirozane-Kishikawa, T., Li, Q., Gabel, H. W., Elewa, A., Baumgartner, B., Rose, D. J., Yu, H., Bosak, S., Sequerra, R., Fraser, A., Mango, S. E., Saxton, W. M., Strome, S., Van Den Heuvel, S., Piano, F., Vandenhaute, J., Sardet, C., Gerstein, M., Doucette-Stamm, L., Gunsalus, K. C., Harper, J. W., Cusick, M. E., Roth, F. P., Hill, D. E., and Vidal, M. (2004) A map of the interactome network of the metazoan C. elegans. *Science* **303,** 540–543
5. Rual, J. F., Venkatesan, K., Hao, T., Hirozane-Kishikawa, T., Dricot, A., Li, N., Berriz, G. F., Gibbons, F. D., Dreze, M., Ayivi-Guedehoussou, N., Klitgord, N., Simon, C., Boxem, M., Milstein, S., Rosenberg, J., Goldberg, D. S., Zhang, L. V., Wong, S. L., Franklin, G., Li, S., Albala, J. S., Lim, J., Fraughton, C., Llamosas, E., Cevik, S., Bex, C., Lamesch, P., Sikorski, R. S., Vandenhaute, J., Zoghbi, H. Y., Smolyar, A., Bosak, S., Sequerra, R., Doucette-Stamm, L., Cusick, M. E., Hill, D. E., Roth, F. P., and Vidal, M. (2005) Towards a proteome-scale map of the human protein-protein interaction network. *Nature* **437,** 1173–1178
6. Stelzl, U., Worm, U., Lalowski, M., Haenig, C., Brembeck, F. H., Goehler, H., Stroedicke, M., Zenkner, M., Schoenherr, A., Koeppen, S., Timm, J., Mintzlaff, S., Abraham, C., Bock, N., Kietzmann, S., Goedde, A., Toksöz, E., Droege, A., Krobitsch, S., Korn, B., Birchmeier, W., Lehrach, H., and Wanker, E. E. (2005) A human protein-protein interaction network: a resource for annotating the proteome. *Cell* **122,** 957–968
7. Tarassov, K., Messier, V., Landry, C. R., Radinovic, S., Serna Molina, M. M., Shames, I., Malitskaya, Y., Vogel, J., Bussey, H., and Michnick, S. W. (2008) An in vivo map of the yeast protein interactome. *Science* **320,** 1465–1470
8. Uetz, P., Giot, L., Cagney, G., Mansfield, T. A., Judson, R. S., Knight, J. R., Lockshon, D., Narayan, V., Srinivasan, M., Pochart, P., Qureshi-Emili, A., Li, Y., Godwin, B., Conover, D., Kalbfleisch, T., Vijayadamodar, G., Yang, M., Johnston, M., Fields, S., and Rothberg, J. M. (2000) A comprehensive analysis of protein-protein interactions in Saccharomyces cerevisiae. *Nature* **403,** 623–627
9. Gingras, A. C., Gstaiger, M., Raught, B., and Aebersold, R. (2007) Analysis of protein complexes using mass spectrometry. *Nat. Rev. Mol. Cell Biol.* **8,** 645–654
10. Köcher, T., and Superti-Furga, G. (2007) Mass spectrometry-based functional proteomics: from molecular machines to protein networks. *Nat. Methods* **4,** 807–815

11. Butland, G., Peregrín-Alvarez, J. M., Li, J., Yang, W., Yang, X., Canadien, V., Starostine, A., Richards, D., Beattie, B., Krogan, N., Davey, M., Parkinson, J., Greenblatt, J., and Emili, A. (2005) Interaction network containing conserved and essential protein complexes in Escherichia coli. *Nature* **433,** 531–537
12. Hu, P., Janga, S. C., Babu, M., Díaz-Mejía, J. J., Butland, G., Yang, W., Pogoutse, O., Guo, X., Phanse, S., Wong, P., Chandran, S., Christopoulos, C., Nazarians-Armavil, A., Nasseri, N. K., Musso, G., Ali, M., Nazemof, N., Eroukova, V., Golshani, A., Paccanaro, A., Greenblatt, J. F., Moreno-Hagelsieb, G., and Emili, A. (2009) Global functional atlas of Escherichia coli encompassing previously uncharacterized proteins. *PLoS Biol.* **7,** e96
13. Gavin, A. C., Aloy, P., Grandi, P., Krause, R., Boesche, M., Marzioch, M., Rau, C., Jensen, L. J., Bastuck, S., Dümpelfeld, B., Edelmann, A., Heurtier, M. A., Hoffman, V., Hoefert, C., Klein, K., Hudak, M., Michon, A. M., Schelder, M., Schirle, M., Remor, M., Rudi, T., Hooper, S., Bauer, A., Bouwmeester, T., Casari, G., Drewes, G., Neubauer, G., Rick, J. M., Kuster, B., Bork, P., Russell, R. B., and Superti-Furga, G. (2006) Proteome survey reveals modularity of the yeast cell machinery. *Nature* **440,** 631–636
14. Gavin, A. C., Bösche, M., Krause, R., Grandi, P., Marzioch, M., Bauer, A., Schultz, J., Rick, J. M., Michon, A. M., Cruciat, C. M., Remor, M., Höfert, C., Schelder, M., Brajenovic, M., Ruffner, H., Merino, A., Klein, K., Hudak, M., Dickson, D., Rudi, T., Gnau, V., Bauch, A., Bastuck, S., Huhse, B., Leutwein, C., Heurtier, M. A., Copley, R. R., Edelmann, A., Querfurth, E., Rybin, V., Drewes, G., Raida, M., Bouwmeester, T., Bork, P., Seraphin, B., Kuster, B., Neubauer, G., and Superti-Furga, G. (2002) Functional organization of the yeast proteome by systematic analysis of protein complexes. *Nature* **415,** 141–147
15. Krogan, N. J., Cagney, G., Yu, H., Zhong, G., Guo, X., Ignatchenko, A., Li, J., Pu, S., Datta, N., Tikuisis, A. P., Punna, T., Peregrín-Alvarez, J. M., Shales, M., Zhang, X., Davey, M., Robinson, M. D., Paccanaro, A., Bray, J. E., Sheung, A., Beattie, B., Richards, D. P., Canadien, V., Lalev, A., Mena, F., Wong, P., Starostine, A., Canete, M. M., Vlasblom, J., Wu, S., Orsi, C., Collins, S. R., Chandran, S., Haw, R., Rilstone, J. J., Gandi, K., Thompson, N. J., Musso, G., St Onge, P., Ghanny, S., Lam, M. H., Butland, G., Altaf-Ul, A. M., Kanaya, S., Shilatifard, A., O'Shea, E., Weissman, J. S., Ingles, C. J., Hughes, T. R., Parkinson, J., Gerstein, M., Wodak, S. J., Emili, A., and Greenblatt, J. F. (2006) Global landscape of protein complexes in the yeast Saccharomyces cerevisiae. *Nature* **440,** 637–643
16. Collins, S. R., Kemmeren, P., Zhao, X. C., Greenblatt, J. F., Spencer, F., Holstege, F. C., Weissman, J. S., and Krogan, N. J. (2007) Toward a comprehensive atlas of the physical interactome of Saccharomyces cerevisiae. *Mol. Cell. Proteomics* **6,** 439–450
17. Ewing, R. M., Chu, P., Elisma, F., Li, H., Taylor, P., Climie, S., McBroom-Cerajewski, L., Robinson, M. D., O'Connor, L., Li, M., Taylor, R., Dharsee, M., Ho, Y., Heilbut, A., Moore, L., Zhang, S., Ornatsky, O., Bukhman, Y. V., Ethier, M., Sheng, Y., Vasilescu, J., Abu-Farha, M., Lambert, J. P., Duewel, H. S., Stewart, I. I., Kuehl, B., Hogue, K., Colwill, K., Gladwish, K., Muskat, B., Kinach, R., Adams, S. L., Moran, M. F., Morin, G. B., Topaloglou, T., and Figeys, D. (2007) Large-scale mapping of human protein-protein interactions by mass spectrometry. *Mol. Syst. Biol.* **3,** 89
18. Glatter, T., Wepf, A., Aebersold, R., and Gstaiger, M. (2009) An integrated workflow for charting the human interaction proteome: insights into the PP2A system. *Mol. Syst. Biol.* **5,** 237
19. Jeronimo, C., Forget, D., Bouchard, A., Li, Q., Chua, G., Poitras, C., Thérien, C., Bergeron, D., Bourassa, S., Greenblatt, J., Chabot, B., Poirier, G. G., Hughes, T. R., Blanchette, M., Price, D. H., and Coulombe, B. (2007) Systematic analysis of the protein interaction network for the human transcription machinery reveals the identity of the 7SK capping enzyme. *Mol. Cell* **27,** 262–274
20. Jeronimo, C., Langelier, M. F., Zeghouf, M., Cojocaru, M., Bergeron, D., Baali, D., Forget, D., Mnaimneh, S., Davierwala, A. P., Pootoolal, J., Chandy, M., Canadien, V., Beattie, B. K., Richards, D. P., Workman, J. L., Hughes, T. R., Greenblatt, J., and Coulombe, B. (2004) RPAP1, a novel human RNA polymerase II-associated protein affinity purified with recombinant wild-type and mutated polymerase subunits. *Mol. Cell. Biol.* **24,** 7043–7058
21. Dull, T., Zufferey, R., Kelly, M., Mandel, R. J., Nguyen, M., Trono, D., and Naldini, L. (1998) A third-generation lentivirus vector with a conditional packaging system. *J. Virol.* **72,** 8463–8471
22. Moffat, J., Grueneberg, D. A., Yang, X., Kim, S. Y., Kloepfer, A. M., Hinkle, G., Piqani, B., Eisenhaure, T. M., Luo, B., Grenier, J. K., Carpenter, A. E., Foo, S. Y., Stewart, S. A., Stockwell, B. R., Hacohen, N., Hahn, W. C., Lander, E. S., Sabatini, D. M., and Root, D. E. (2006) A lentiviral RNAi library for human and mouse genes applied to an arrayed viral high-content screen. *Cell* **124,** 1283–1298
23. Zufferey, R., Nagy, D., Mandel, R. J., Naldini, L., and Trono, D. (1997) Multiply attenuated lentiviral vector achieves efficient gene delivery in vivo. *Nat. Biotechnol.* **15,** 871–875
24. Walhout, A. J., Temple, G. F., Brasch, M. A., Hartley, J. L., Lorson, M. A., van den Heuvel, S., and Vidal, M. (2000) GATEWAY recombinational cloning: application to the cloning of large numbers of open reading frames or ORFeomes. *Methods Enzymol.* **328,** 575–592
25. Chen, G. I., Tisayakorn, S., Jorgensen, C., D'Ambrosio, L. M., Goudreault, M., and Gingras, A. C. (2008) PP4R4/KIAA1622 forms a novel stable cytosolic complex with phosphoprotein phosphatase 4. *J. Biol. Chem.* **283,** 29273–29284
26. Nagy, A., Rossant, J., Nagy, R., Abramow-Newerly, W., and Roder, J. C. (1993) Derivation of completely cell culture-derived mice from early-passage embryonic stem cells. *Proc. Natl. Acad. Sci. U.S.A.* **90,** 8424–8428
27. Chen, G. I., and Gingras, A. C. (2007) Affinity-purification mass spectrometry (AP-MS) of serine/threonine phosphatases. *Methods* **42,** 298–305
28. Florens, L., Carozza, M. J., Swanson, S. K., Fournier, M., Coleman, M. K., Workman, J. L., and Washburn, M. P. (2006) Analyzing chromatin remodeling complexes using shotgun proteomics and normalized spectral abundance factors. *Methods* **40,** 303–311
29. Woltjen, K., Michael, I. P., Mohseni, P., Desai, R., Mileikovsky, M., Hämäläinen, R., Cowling, R., Wang, W., Liu, P., Gertsenstein, M., Kaji, K., Sung, H. K., and Nagy, A. (2009) piggyBac transposition reprograms fibroblasts to induced pluripotent stem cells. *Nature* **458,** 766–770
30. Schmidt, T. G., and Skerra, A. (2007) The Strep-tag system for one-step purification and high-affinity detection or capturing of proteins. *Nat. Protoc.* **2,** 1528–1535
31. Giannone, R. J., McDonald, W. H., Hurst, G. B., Huang, Y., Wu, J., Liu, Y., and Wang, Y. (2007) Dual-tagging system for the affinity purification of mammalian protein complexes. *BioTechniques* **43,** 296, 298, 300 passim
32. Wepf, A., Glatter, T., Schmidt, A., Aebersold, R., and Gstaiger, M. (2009) Quantitative interaction proteomics using mass spectrometry. *Nat. Methods* **6,** 203–205
33. Rozenblatt-Rosen, O., Hughes, C. M., Nannepaga, S. J., Shanmugam, K. S., Copeland, T. D., Guszczynski, T., Resau, J. H., and Meyerson, M. (2005) The parafibromin tumor suppressor protein is part of a human Paf1 complex. *Mol. Cell. Biol.* **25,** 612–620
34. Zhu, B., Mandal, S. S., Pham, A. D., Zheng, Y., Erdjument-Bromage, H., Batra, S. K., Tempst, P., and Reinberg, D. (2005) The human PAF complex coordinates transcription with events downstream of RNA synthesis. *Genes Dev.* **19,** 1668–1673
35. Chaudhary, K., Deb, S., Moniaux, N., Ponnusamy, M. P., and Batra, S. K. (2007) Human RNA polymerase II-associated factor complex: dysregulation in cancer. *Oncogene* **26,** 7499–7507
36. Kim, J., Guermah, M., and Roeder, R. G. (2010) The human PAF1 complex acts in chromatin transcription elongation both independently and cooperatively with SII/TFIIS. *Cell* **140,** 491–503
37. Peterlin, B. M., and Price, D. H. (2006) Controlling the elongation phase of transcription with P-TEFb. *Mol. Cell* **23,** 297–305
38. Narita, T., Yamaguchi, Y., Yano, K., Sugimoto, S., Chanarat, S., Wada, T., Kim, D. K., Hasegawa, J., Omori, M., Inukai, N., Endoh, M., Yamada, T., and Handa, H. (2003) Human transcription elongation factor NELF: identification of novel subunits and reconstitution of the functionally active complex. *Mol. Cell. Biol.* **23,** 1863–1873
39. Narita, T., Yung, T. M., Yamamoto, J., Tsuboi, Y., Tanabe, H., Tanaka, K., Yamaguchi, Y., and Handa, H. (2007) NELF interacts with CBC and participates in 3′ end processing of replication-dependent histone mRNAs. *Mol. Cell* **26,** 349–365
40. Liedtke, M., and Cleary, M. L. (2009) Therapeutic targeting of MLL. *Blood* **113,** 6061–6068
41. Patel, A., Dharmarajan, V., Vought, V. E., and Cosgrove, M. S. (2009) On the mechanism of multiple lysine methylation by the human mixed lineage leukemia protein-1 (MLL1) core complex. *J. Biol. Chem.* **284,**

24242–24256
42. Reisman, D., Glaros, S., and Thompson, E. A. (2009) The SWI/SNF complex and cancer. *Oncogene* **28,** 1653–1668
43. Smith, J. R., Clarke, P. A., de Billy, E., and Workman, P. (2009) Silencing the cochaperone CDC37 destabilizes kinase clients and sensitizes cancer cells to HSP90 inhibitors. *Oncogene* **28,** 157–169
44. Cho, Y. W., Hong, T., Hong, S., Guo, H., Yu, H., Kim, D., Guszczynski, T., Dressler, G. R., Copeland, T. D., Kalkum, M., and Ge, K. (2007) PTIP associates with MLL3- and MLL4-containing histone H3 lysine 4 methyltransferase complex. *J. Biol. Chem.* **282,** 20395–20406
45. Wang, X., Lou, Z., Dong, X., Yang, W., Peng, Y., Yin, B., Gong, Y., Yuan, J., Zhou, W., Bartlam, M., Peng, X., and Rao, Z. (2009) Crystal structure of the C-terminal domain of human DPY-30-like protein: A component of the histone methyltransferase complex. *J. Mol. Biol.* **390,** 530–537
46. Lee, J. H., and Skalnik, D. G. (2005) CpG-binding protein (CXXC finger protein 1) is a component of the mammalian Set1 histone H3-Lys4 methyltransferase complex, the analogue of the yeast Set1/COMPASS complex. *J. Biol. Chem.* **280,** 41725–41731
47. Wong, D. C., Wong, K. T., Nissom, P. M., Heng, C. K., and Yap, M. G. (2006) Targeting early apoptotic genes in batch and fed-batch CHO cell cultures. *Biotechnol. Bioeng.* **95,** 350–361
48. Ruepp, A., Waegele, B., Lechner, M., Brauner, B., Dunger-Kaltenbach, I., Fobo, G., Frishman, G., Montrone, C., and Mewes, H. W. (2010) CORUM: the comprehensive resource of mammalian protein complexes—2009. *Nucleic Acids Res.* **38,** D497–D501
49. Rowland, B. D., and Peeper, D. S. (2006) KLF4, p21 and context-dependent opposing forces in cancer. *Nat. Rev. Cancer* **6,** 11–23
50. Takahashi, K., Tanabe, K., Ohnuki, M., Narita, M., Ichisaka, T., Tomoda, K., and Yamanaka, S. (2007) Induction of pluripotent stem cells from adult human fibroblasts by defined factors. *Cell* **131,** 861–872
51. Takahashi, K., and Yamanaka, S. (2006) Induction of pluripotent stem cells from mouse embryonic and adult fibroblast cultures by defined factors. *Cell* **126,** 663–676
52. Rigaut, G., Shevchenko, A., Rutz, B., Wilm, M., Mann, M., and Séraphin, B. (1999) A generic protein purification method for protein complex characterization and proteome exploration. *Nat. Biotechnol.* **17,** 1030–1032
53. Bürckstümmer, T., Bennett, K. L., Preradovic, A., Schütze, G., Hantschel, O., Superti-Furga, G., and Bauch, A. (2006) An efficient tandem affinity purification procedure for interaction proteomics in mammalian cells. *Nat. Methods* **3,** 1013–1019
54. Blagoev, B., Kratchmarova, I., Ong, S. E., Nielsen, M., Foster, L. J., and Mann, M. (2003) A proteomics strategy to elucidate functional protein-protein interactions applied to EGF signaling. *Nat. Biotechnol.* **21,** 315–318
55. Ho, L., Jothi, R., Ronan, J. L., Cui, K., Zhao, K., and Crabtree, G. R. (2009) An embryonic stem cell chromatin remodeling complex, esBAF, is an essential component of the core pluripotency transcriptional network. *Proc. Natl. Acad. Sci. U.S.A.* **106,** 5187–5191
56. Ho, L., Ronan, J. L., Wu, J., Staahl, B. T., Chen, L., Kuo, A., Lessard, J., Nesvizhskii, A. I., Ranish, J., and Crabtree, G. R. (2009) An embryonic stem cell chromatin remodeling complex, esBAF, is essential for embryonic stem cell self-renewal and pluripotency. *Proc. Natl. Acad. Sci. U.S.A.* **106,** 5181–5186
57. Kidder, B. L., Palmer, S., and Knott, J. G. (2009) SWI/SNF-Brg1 regulates self-renewal and occupies core pluripotency-related genes in embryonic stem cells. *Stem Cells* **27,** 317–328